J. Appl. Cryst. (1999). **32**, 761–769

Structure of sodium *para*-hydroxybenzoate, $NaO_2C–C_6H_4OH$ by powder diffraction: application of a phenomenological model of anisotropic peak width

R. E. Dinnebier,[a]* R. Von Dreele,[b] P. W. Stephens,[c] S. Jelonek[d] and J. Sieler[d]

[a]*Laboratory of Crystallography, University of Bayreuth, D-95440 Bayreuth, Germany,* [b]*LANSCE, MS-H805, Los Alamos National Laboratory, Los Alamos, NM 87545, USA,* [c]*Department of Physics and Astronomy, State University of New York, Stony Brook, New York 11794-3800, USA, and* [d]*Institute of Inorganic Chemistry, University of Leipzig, D-04103 Leipzig, Germany. E-mail: robert.dinnebier@uni-bayreuth.de*

(*Received 14 January 1999; accepted 12 April 1999*)

Abstract

The *ab initio* structure solution of sodium *para*-hydroxybenzoate from high-resolution X-ray powder diffraction data is reported. The compound is of interest with respect to understanding the mechanism of Kolbe–Schmitt type reactions. It crystallizes in space group $P2_1$, $Z = 2$, with unit-cell parameters $a = 16.0608$ (3), $b = 5.38291$ (9), $c = 3.63834$ (6) Å, $\beta = 92.8692$ (5)° and $V = 314.153$ Å^3. The compound consists of layers of distorted NaO_6 prisms perpendicular to the a axis and phenol rings perpendicular to these layers pointing up and down. The molecular structure is held together by van der Waals forces between the phenyl groups of different layers and additional hydrogen-bridge bonding between the phenolate oxygen atoms. The sample showed powder peak widths which are not a smooth function of diffraction angle; a recently implemented phenomenological model was able to describe this effect sufficiently well to obtain excellent Rietveld fits to the data. The accuracy of modeling the data makes this one of the rare cases where the position of a hydrogen atom could be unambiguously determined by powder techniques.

1. Introduction

The carboxylation of sodium phenolate, known as Kolbe–Schmitt synthesis (Kolbe, 1874), leads to two main reaction products: sodium *ortho*-hydroxybenzoate, also known as sodium salicylate, and sodium *para*-hydroxybenzoate. The reaction is still one of the most important industrial solid-state reactions, with many applications in the synthesis of pigments, fertilizers and pharmaceuticals, such as aspirin (Behr, 1985; *Brockhaus ABC Chemie*, 1971). Although the reaction has been known since the middle of the previous century (Kolbe & Lautermann, 1860), and despite its importance, its mechanism and the crystal structures of its products are still unknown. Many models for the reaction mechanism have been published (Hales *et al.*, 1954). The types and the amounts of the reaction products are strongly influenced by the reaction conditions, namely temperature, pressure, time, type of alkaline cation and solvent (*e.g.* Lindsey & Jeskey, 1957, and references therein). Under typical reaction conditions (393 K, 5 atm), the carboxylation of dry sodium phenolate leads to an almost quantitative yield of sodium salicylate (Lindsey & Jeskey, 1957). An increase in the production of sodium *para*-hydroxybenzoate can be achieved at lower temperatures or by the chelation of sodium phenoxide with polyethers (Sakakibara & Haraguchi, 1980).

We have begun a major investigation to solve the crystal structures of the substances related to Kolbe–Schmitt type reactions in order to gain further insight into their mechanism. The structures of the reactants have recently been solved using single-crystal X-ray diffraction and high-resolution X-ray powder diffraction (Dinnebier *et al.*, 1997). Here we report the crystal structure of sodium *para*-hydroxybenzoate from high-resolution X-ray powder diffraction data. Since this compound is a possible intermediate or product of the Kolbe–Schmitt synthesis, its structure is of particular interest for future *in situ* investigations with temperature- and time-resolved powder diffraction.

Since the early work of Hugo Rietveld (Rietveld, 1969), structure refinement and also structure determination from powder data have become more and more important (*e.g.* Harris & Tremayne, 1996; Langford & Louër, 1996; Masciocchi & Sironi, 1997; Poojary & Clearfield, 1997). One major obstacle in the development of this method was that the reflection line shape obtained by X-ray powder diffraction is much more complicated than in the case of neutron diffraction, and it took many years before a generally applicable and physically meaningful description was found. Important contributions have been the parametrization of the Voigt function (Thompson, Cox & Hastings, 1987) and the description of the asymmetry due to axial divergence (Finger *et al.*, 1994). Nowadays, it is often possible to describe the entire profile of a synchrotron powder pattern with only four adjustable parameters. On the other hand, the especially high resolution of synchrotron radiation revealed another problem which hinders a

satisfactory description of the peak profile of real powders: the fact that for many samples, the diffraction peak width is not a smooth function of diffraction angle. Most of the available Rietveld programs produce unacceptable fits when presented with this anisotropic broadening (in the three-dimensional diffraction space); see Le Bail (1992) for a useful review of previous attempts. These treatments offer different numbers of additional adjustable profile parameters, but often lack a connection with any plausible microscopic source of anisotropic broadening and frequently do not even obey the conditions imposed by crystallographic symmetry.

The title compound shows severe anisotropic broadening which could not be modeled by any of the hitherto available algorithms. This motivated one of us (Stephens, 1999) to develop an empirical model of anisotropic broadening due to correlated variations in lattice metric parameters, which extends and corrects previous work by Thompson, Reilly & Hastings (1987) and Rodríguez-Carvajal *et al.* (1991). This has been implemented in the program *GSAS* (Larson & Von Dreele, 1994) used in the present work to refine the structure. Popa (1998) has independently published a similar model, but without an explicit experimental realisation. There has been some progress in providing a microscopic interpretation of this model (Ungar & Tichy, 1999), but so far its main value is in improving the ability of a calculated line shape to match experimental data, thereby increasing the reliability of a Rietveld refinement. In the present case, this improvement was sufficiently dramatic that the data could be used to locate the position of the hydrogen atom of the phenol hydroxy group by difference Fourier analysis of powder data. This hydrogen-atom position was then subsequently included in the Rietveld refinement of the structure.

2. Experimental

2.1. *Materials*

All manipulations of solvents and substances were carried out in dry argon using standard Schlenk and vacuum techniques. Tetrahydrofuran (thf) was purified and dried according to the standard procedures. 5.7 g of sodium (0.25 mol) was covered with thf and heated until melting under rapid stirring. A solution of 34.5 g of *p*-hydroxybenzoic acid (0.25 mol) in 100 ml of thf was added dropwise over 1 h to the stirred finely dispersed sodium. After completion of the reaction, half of the solvent was evaporated. A white powder precipitated, which was filtered off and dried at 353 K in a Schlenk vessel, from which it was transferred to glass capillaries in a glove box under argon atmosphere.

Table 1. *Lattice parameters and selected details of refinements of sodium para-hydroxybenzoate*

R_p, R_{wp}, $R(F)$ and $R(F^2)$ refer to the Rietveld criteria of fit for profile, weighted profile and structure factor, respectively, defined by Langford & Louër (1996).

a (Å)	16.0608 (3)
b (Å)	5.38291 (9)
c (Å)	3.63834 (7)
β (°)	92.8692 (5)
V (Å^3)	314.153 (9)
V/Z (Å^3)	157.077
Z	2
Formula weight (g mol^{-1})	320.208
Space group	$P2_1$
Calculated density (g cm^3)	1.693
R_p (%)	5.24
R_{wp} (%)	7.16
$R(F)$ (%)	4.48
$R(F^2)$ (%)	5.98
No. of reflections	418
No. of refined variables	39

2.2. *Powder X-ray diffraction experiments*

For the X-ray powder diffraction experiments, the sample was sealed in a glass capillary of 0.7 mm diameter. High-resolution powder diffraction data were collected at the SUNY X3B1 beamline at the National Synchrotron Light Source, Brookhaven National Laboratory. X-rays of wavelength 1.14750 (2) Å were selected by a double Si(111) monochromator. Wavelengths and the zero point have been determined from eight well defined reflections of the NBS1976 flat-plate alumina standard. The diffracted beam was analysed with a Ge(111) crystal and detected with an Na(Tl)I scintillation counter with a pulse-height discriminator in the counting chain. The incoming beam was monitored by an ion chamber for normalization of the decay of the primary beam. In this parallel-beam configuration, the resolution is determined by the analyser crystal instead of by slits. Data were recorded at room temperature for 4.3 s at each 2θ in steps of 0.005° from 3 to 73.195°.

Although θ scans did not show serious crystallite size effects, the sample was rocked around θ for 5° during measurement for better particle statistics. Low-angle diffraction peaks showed a strong asymmetry due to axial divergence and had a full width at half-maximum (FWHM) of 0.012° in 2θ, which is close to the resolution of the spectrometer.

The diffraction pattern could be indexed on the basis of a monoclinic lattice with lattice parameters as given in Table 1 (Visser, 1969). The possible space groups were $P2_1$ and $P2_1/m$. The number of formula units per unit cell (Z) directly follows from geometrical considerations. A Le Bail fit (Le Bail *et al.*, 1988) using the program *FULLPROF* (Rodríguez-Carvajal, 1990) allowed extraction of 416 integrated intensities up to 72.91° in 2θ. It should be noted that despite the large number of well resolved peaks, the quality of the Le Bail

fit was rather bad because of the strong anisotropy of the FWHM. Despite using the uniaxial strain model with the (110) direction as the broadening axis, the weighted profile R factor was unsatisfactorily high (23.9%).

The obtained integrated intensities were used as input to the direct-methods program *SIRPOW*92 (Cascarano *et al.*, 1992). Using $P2_1/m$, it was possible to detect the entire molecule without hydrogen atoms. Since the arrangement of the molecules restricted by the mirror plane seemed quite unfavourable, and first attempts to refine the structure by Rietveld analysis (Rietveld, 1969) did not converge, the space group was changed to $P2_1$. Subsequent refinements confirmed $P2_1$ as the correct space group.

Although the structure seemed to be chemically correct at this stage of the refinement, the Rietveld plot could not be regarded as 'publishable' because of the large deviations between the observed and calculated profiles, caused by the anisotropy in the FWHM. A plot showing the FWHM of single or only partly overlapping peaks, obtained by single-peak fitting, *versus* diffraction angle 2θ clearly shows the strong deviations from a smooth function. The FWHM of neighbouring peaks varies by a factor of up to 4 (see Fig. 1 of Stephens, 1999).

3. Anisotropic broardening

The following model was used for the distribution of powder diffraction peak widths. Each crystallite is regarded as having its own lattice parameters, with a multi-dimensional distribution throughout the powder sample. The width of each reflection can be expressed in terms of moments of this distribution, which leads naturally to parameters that can be varied to achieve optimal fits. Interested readers are referred to the paper by Stephens (1999) for further description of the model and the derivation of the line shape used here.

We define d^*_{hkl} to be the inverse of the d spacing of the (hkl) reflection. Then d^{*2} is bilinear in the Miller indices and so can be expanded in terms related to the covariances of the distribution of lattice metrics. This leads to an expression in which the variance of d^{*2} is a sum of 15 different combinations of Miller indices in the fourth order. Imposing the symmetry of the monoclinic lattice [*e.g.* reflections (hkl), $(h\bar{k}l)$, $(\bar{h}k\bar{l})$ and $(\bar{h}\bar{k}\bar{l})$ are equivalent] reduces the number of independent terms to the following nine:

$$\begin{aligned} S^2 = {} & S_{400}h^4 + S_{040}k^4 + S_{004}l^4 \\ & + 3(S_{220}h^2k^2 + S_{202}h^2l^2 + S_{022}k^2l^2) \\ & + 2(S_{103}hl^3 + S_{301}h^3l) + 3S_{121}hk^2l. \end{aligned} \quad (1)$$

The anisotropic strain contribution to the angular width in 2θ of the reflection is given by

$$\delta 2\theta = (360/\pi)(\delta d/d)\tan\theta, \quad (2)$$

where

$$\delta d/d = \pi(S^2)^{1/2}/18\,000\, d^*_{hkl}. \quad (3)$$

Here, we regard the parameters S_{HKL} as free parameters, to be chosen to obtain the best fit between model and experiment. The anisotropic broadening has both Gaussian and Lorentzian components; we have found it important to include both, in order to obtain an acceptable fit to the diffraction data. We have therefore introduced another interpolation parameter, ζ, so that the half width at half-maximum of the Lorentzian component is given by $X + \zeta\delta 2\theta$, and the variance of the Gaussian component of the line shape is given by

$$[U\tan^2\theta + V\tan\theta + W + P/\cos\theta + (1-\zeta)^2\delta 2\theta^2]^{1/2}. \quad (4)$$

4. Rietveld refinements

The Rietveld refinements were calculated using the program package *GSAS* (Larson & Von Dreele, 1994) (Fig. 1). The peak profile function was modeled using a convolution of the pseudo-Voigt function (Thompson, Cox & Hastings, 1987) with the asymmetry function described by Finger *et al.* (1994), which accounts for the asymmetry due to axial divergence, leading to a markedly improved fit and therefore better profile R factors. A small shift of diffraction peaks across the spectrum was detected, which we attributed to a drift of the X-ray wavelength, presumably due to heating of the monochromator. This effect could be satisfactorily described by refining an additional $\sin\theta$ term in addition to the zero point. For the background function, a first estimate was piecemeal interpolated from manually chosen points of the spectrum; in later stages of refinement, it was supplemented by a four-term cosine series.

To account for the strong anisotropy in the half width of the reflections, we used the model by Stephens (1999) described above, which has recently been implemented in *GSAS* (Von Dreele, 1998). Refinement of this model was performed stepwise. Initially only the S_{400}, S_{040} and S_{004} coefficients were refined; initial values were zero and the mixing coefficient, ζ, was set to 0.75. After convergence, the S_{220}, S_{202} and S_{022} terms were added to the refinement followed by the terms S_{301}, S_{103} and S_{121}. Finally, the mixing coefficient, ζ, was allowed to vary with the other terms. This procedure resulted in a smooth minimization; attempts to refine all S_{HKL} and ζ simultaneously from the start generally failed to converge cleanly. For the purpose of comparison, two Rietveld plots are given: one shows the result of a refinement in which the anisotropic peak width model has been used (Fig. 1*b*); the second one (otherwise identical) was prepared without this model (Fig. 1*a*).

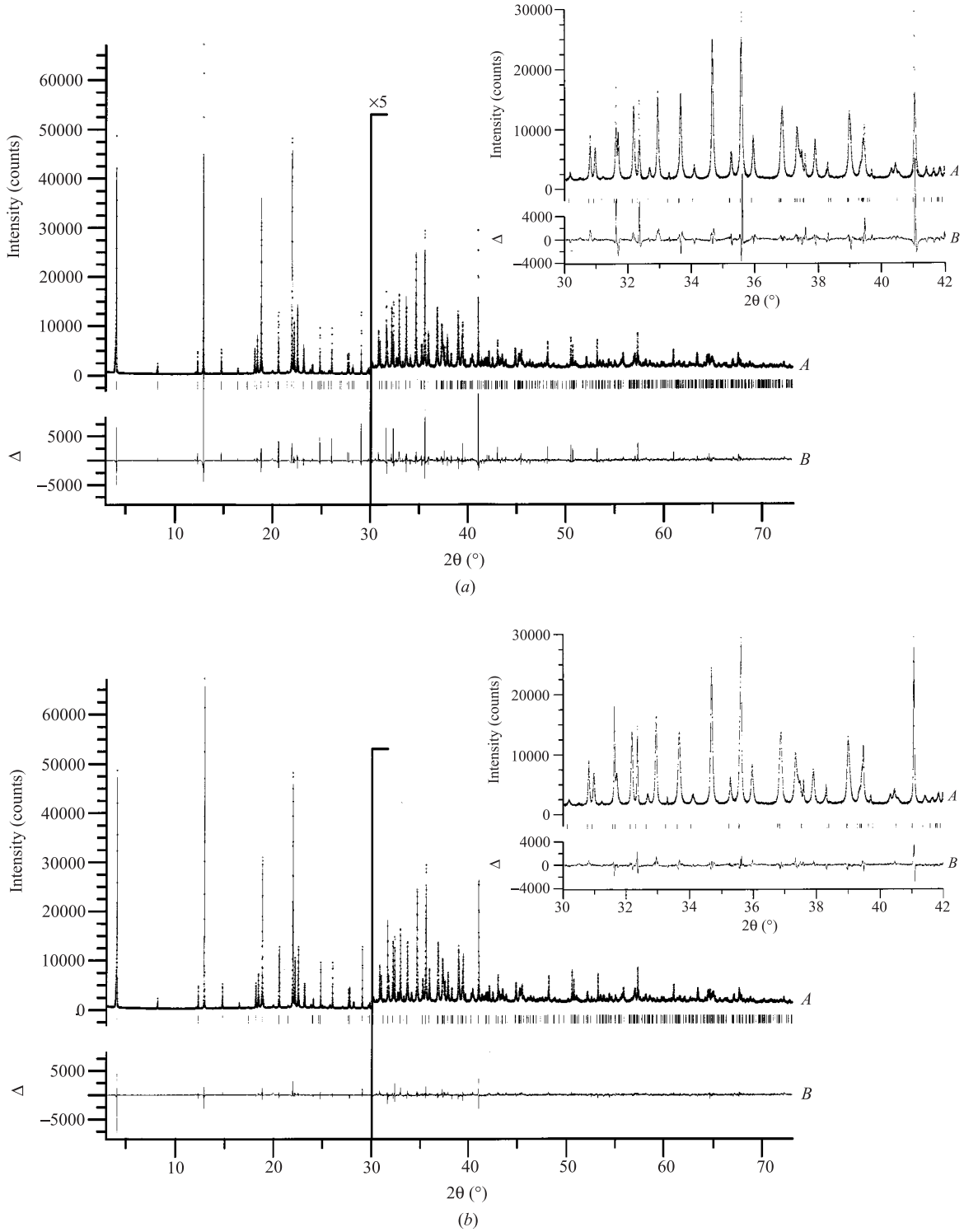

Fig. 1. Scattered X-ray intensity for sodium *para*-hydroxybenzoate at T = 295 K as a function of diffraction angle 2θ. Shown are the observed pattern (diamonds), the best Rietveld fit profile, the difference curve between the observed and the calculated profile, and the reflection markers (vertical bars). λ = 1.14750 (2) Å. The higher angle part starting at 30° in 2θ is enlarged by a factor of five. The inset shows the expanded region from 30 to 42° in 2θ. The Rietveld plot in (*a*) shows the refinement without the anisotropic broadening model. The R values are R_p = 10.26%, R_{wp} = 17.75%, $R(F)$ = 5.24%, $R(F^2)$ = 7.74%. The Rietveld plot in (*b*) shows the refinement with the anisotropic broadening model. The R values are R_p = 5.24%, R_{wp} = 7.16%, $R(F)$ = 4.48%, $R(F^2)$ = 5.98%.

In order to stabilize the refinement, two rigid bodies, one for the phenyl ring and another one for the carboxyl group, were used. It was not considered necessary in this work to determine the internal details of these molecular moieties because they have well established structures. A comparison of similar *para*-substituted benzene ring compounds in the literature [*viz*. *p*-hydroxybenzoic acid monohydrate (Colapietro, Domenicano & Marciante, 1979), *p*-nitrobenzoic acid (Colapietro & Domenicano, 1977), *p*-methoxybenzoic acid (Colapietro & Domenicano, 1978), *p*-fluorobenzoic acid (Colapietro, Domenicano & Ceccarini, 1979), *p*-hydroxybenzoic acid and *p*-hydroxybenzoic acid–acetone complex (Heath *et al.*, 1992), and potassium hydrogen di-*p*-hydroxybenzoate hydrate (Manojlovic, 1968)] shows that the deviations from planarity as well as the deviations from hexagonal symmetry for both groups are in the range of the standard uncertainties derived from the powder data. The rigid bodies were set up in a such a way that several intrameolecular bond distances remained as refinable parameters, and only the bond lengths and angles of the C_6 ring were kept fixed. In addition, the two rigid bodies were constrained in such a way that only the dihedral angle between the phenyl ring and the carboxyl group remained as a free parameter. This important step reduced the number of independent positional parameters from 42 to 13 (three rotational, three translational, six bond lengths, one dihedral angle). After convergence, all intramolecular distances agreed well with those from single-crystal structure determinations of related compounds in the literature (cited above).

Surprisingly, the computation of the three-dimensional difference electron density clearly revealed a peak with 0.8 e Å^{-3}, exactly at the expected position for the missing hydroxy hydrogen atom (Fig. 2). This hydrogen atom was added to the list of atoms and its position could be refined. The displacement parameter has been assigned an arbitrary value. This is one of the rare cases where the position of a hydrogen atom was found *and* refined from powder data alone (*e.g.* Smith *et al.*, 1988; Schmidt *et al.*, 1998), whereas their positions have been inferred in previous experiments (*e.g.*, Lengauer *et al.*, 1995).

As a final test for the correctness of the molecular geometry, all atomic positions were refined independently after excluding the hydrogen atoms from the refinement. The positions of all non-hydrogen atoms remained close to their original positions but the weighted profile *R* factor increased by several percent, demonstrating the measurable contribution of hydrogen atoms to the powder pattern profile, in agreement with previous reports (*e.g.* Lightfoot *et al.*, 1993).

The *R* values are listed in Table 1. The coordinates (using rigid bodies) are given in Table 2. Selected intra- and intermolecular distances are given in Table 3. The refined profile parameters as defined in the anisotropic broadening section (§3) are given in Table 4. A graphical representation of the three-dimenisonal strain distribution using the refined S_{HKL} values is given in Fig. 3.†

5. Description of the structure

The structure is based on layers of NaO_6 polyhedra perpendicular to the *a* axis and phenyl rings perpendicular to those layers pointing along the *a* axis (Fig. 4). Each sodium atom is coordinated to six oxygen atoms in the form of a distorted trigonal prism, similar to that in Na_2SO_4-V (thenardite) (Mehrotra *et al.*, 1978) (Fig. 5). The NaO_6 prisms are connected quite unfavourably *via*

† Lists of structure factors and the numerical intensity of each point of the room-temperature profile of sodium *p*-hydroxybenzoate, along with the output tables generated by the Rietveld refinement program *GSAS*, have been deposited in the IUCr electronic archives (Reference: HN0100). Services for accessing these data are described at the back of the journal.

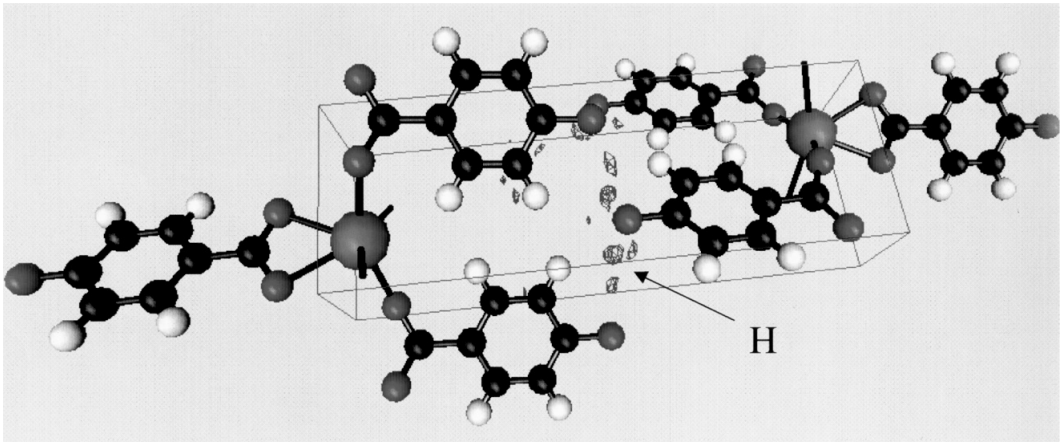

Fig. 2. Three-dimensional difference Fourier plot of sodium *para*-hydroxybenzoate in space group $P2_1$ after applying the anisotropic FWHM model. The missing hydroxy hydrogen atoms are clearly visible between the hydroxy oxygen atoms.

Table 2. *Positional parameters and U^i ($Å^2 \times 10^3$) of sodium para-hydroxybenzoate at 295 K*

Standard uncertainties are a factor of six larger than Rietveld statistical estimates, as discussed by Langford & Louër (1996). The values of the displacement parameter are constrained to be equal for the entire rigid body and were set to an arbitrary value for the hydroxy hydrogen atom.

	x	y	z	U^i		x	y	z	U^i
Na	0.9474 (4)	0.8031	0.257 (2)	36 (3)	H1	0.610 (2)	0.601 (6)	0.588 (5)	21 (1)
O1	0.5255 (6)	0.243 (2)	0.871 (2)	21 (1)	H2	0.636 (1)	−0.084 (6)	0.087 (5)	21 (1)
C1	0.6106 (4)	0.256 (2)	0.842 (1)	21 (1)	H3	0.757 (1)	0.624 (6)	0.538 (5)	21 (1)
C2	0.6458 (4)	0.463 (2)	0.681 (2)	21 (1)	H4	0.783 (2)	−0.061 (6)	0.037 (5)	21 (1)
C3	0.6613 (3)	0.063 (2)	0.973 (2)	21 (1)	H	0.49 (1)	0.09 (2)	0.03 (4)	50
C4	0.7317 (3)	0.477 (2)	0.652 (2)	21 (1)					
C5	0.7472 (3)	0.077 (2)	0.943 (3)	21 (1)					
C6	0.7824 (3)	0.284 (2)	0.783 (1)	21 (1)					
C7	0.8741 (3)	0.298 (2)	0.752 (1)	21 (1)					
O2	0.9091 (5)	0.511 (3)	0.692 (3)	21 (1)					
O3	0.9179 (6)	0.104 (3)	0.83 (3)	21 (1)					

six out of nine edges with neighbouring prisms, forming an infinite layer. The bond distances between the sodium and oxygen atoms are 2.33 (1) to 2.64 (1) Å, comparable to those of other compounds containing NaO_6 prisms, such as Na_2SO_4 (2.335–2.535 Å) and Na_2SeO_4 (2.330–2.592 Å) (Mehrotra *et al.*, 1978). The base of the NaO_6 prism defines a perfect plane, whereas the 'roof atoms' show small deviations in the height relative to the basal plane (Fig. 5*b*). There is no interaction between the sodium atom and the π system of the phenyl ring, in contrast to the structures of sodium phenolate and sodium phenolate diphenol (Kunert *et al.*, 1997; Jörchel & Sieler, 1994).

The phenol rings extend perpendicularly from both sides of the layer formed by the NaO_6 prisms in an alternating way (Fig. 4). They are rotated in different directions by $\pm 29.1\ (3)^\circ$ relative to the *ab* plane. The carboxyl group is twisted by $17.5\ (3)^\circ$ relative to the phenol ring. This dihedral angle is somewhat larger than observed in other substituted benzoic acids (1.8–5.0°) and one of their salts (9.5°). This can be explained by steric requirements of the sodium atom, which result in the connection of the NaO_6 prism, and which are probably one of the causes for the severe strain evident in the anisotropic powder diffraction profile broadening (Figs. 1 and 3).

The molecular structure is held together by van der Waals forces between phenyl groups of different layers and additional hydrogen-bridge bonding between the phenolate oxygen atoms.

All intra- and intermolecular distances agree well with those of the literature (Table 3).

Table 3. *Selected bond-distance ranges and intramolecular distances of sodium para-hydroxybenzoate as compared to literature values (Å)*

Standard uncertainties are a factor of six larger than Rietveld statistical estimates, as discussed by Langford & Louër (1996).

	Sodium *p*-hydroxybenzoate	Related compounds
Na···Na (short)	3.595 (5)	–
Na···O	2.34 (1)–2.64 (1)	2.330–2.592
Na···C (shortest)	2.869 (6)	–
Na···H (shortest)	2.81 (4)	–
C—O (phenolic)	1.38 (1)	1.357–1.385
C—O (carboxyl)	1.26 (2), 1.30 (2)	1.228, 1.322
C—C (phenyl)	1.391 (4)	1.385–1.395
C(phenyl)—C(carboxyl)	1.485 (6)	1.475
C—H (phenyl)	0.99 (4)	0.98
H···H (shortest interchain)	2.2 (2)	–
O···O (shortest carboxyl)	2.22 (1)	–
O···O (shortest phenolate)	2.979 (6)	–
O—H	1.189 (2)	0.84
H···O (hydrogen bond)	1.9 (1)	1.73–2.01

Table 4. *Refined profile and strain parameters corresponding to profile function No. 4 in the Rietveld refinement program GSAS*

$U = V = W$	0
P (cdeg^2)	0.1
X (cdeg)	0.432
ζ	0.6657
*S*400	0.000224 (7)
*S*040	0.0222 (9)
*S*004	1.64 (2)
*S*220	0.0084 (2)
*S*202	0.274 (4)
*S*022	0.433 (8)
*S*301	0.0203 (8)
*S*103	0.08 (1)
*S*121	0.0224 (8)

6. Conclusions

The increased use of synchrotron powder data reveals structural defects which often influence the shape of the line profile, and for which adequate descriptions must be found. In the present case, the application of an empirical model for the description of anisotropic peak width caused by strain broadening leads to a strong improvement in the description of the line profile as used in Le Bail and Rietveld fits. The importance of a physically meaningful model lies especially in the correct prediction of the peak width of overlapping reflections, allowing for a better peak decomposition in a Le Bail fit and for a more accurate Rietveld refinement.

The latter allows previously inaccessible structural details to be revealed, as in the present case, the determination of the strain distribution and the unambiguous determination of the position of a hydrogen atom by powder techniques.

It should be noted that the use of rigid bodies involving satellite groups is crucial to stabilize the refinement of flexible molecular structures from powder data, since meaningless changes of positional parameters will generally be avoided.

Research was carried out in part at the National Synchrotron Light Source at Brookhaven National Laboratory, which is supported by the US Department of Energy, Division of Materials Sciences and Division of Chemical Sciences. The SUNY X3 beamline at NSLS

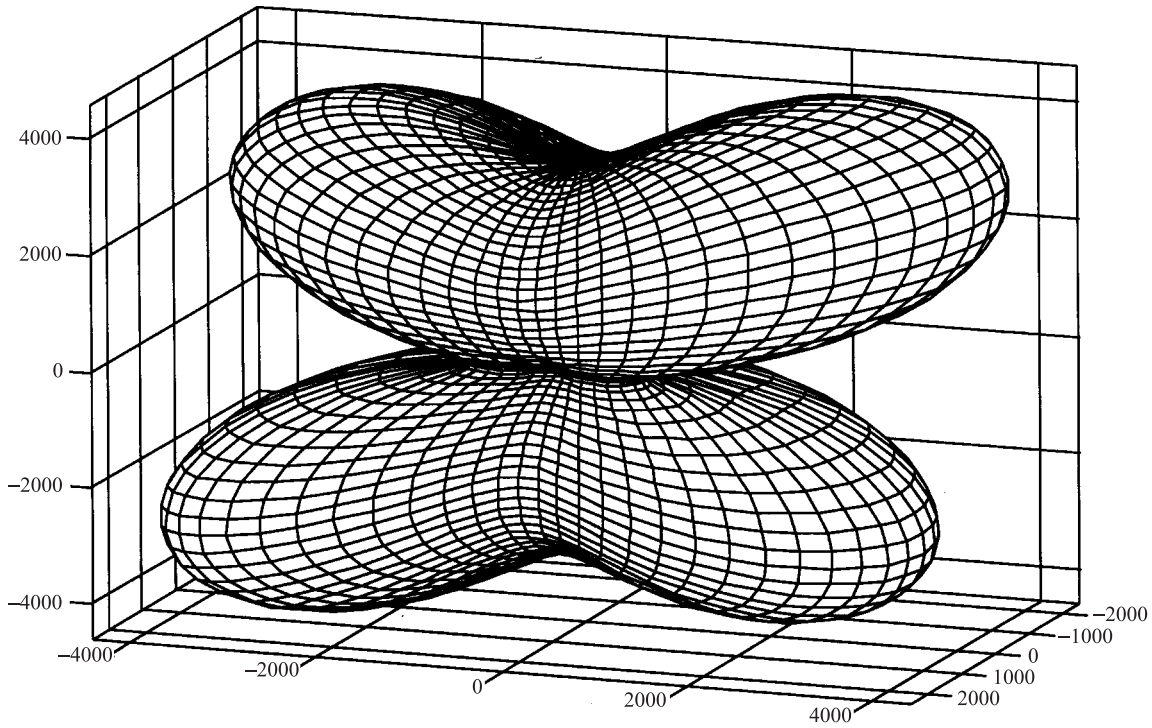

Fig. 3. Three-dimensional strain distribution of sodium *para*-hydroxybenzoate. The *x* axis is horizontal, the *z* axis vertical and the *y* axis out of the plane of the paper. The scale is in $\delta d/d \times 10^{-6}$ strain.

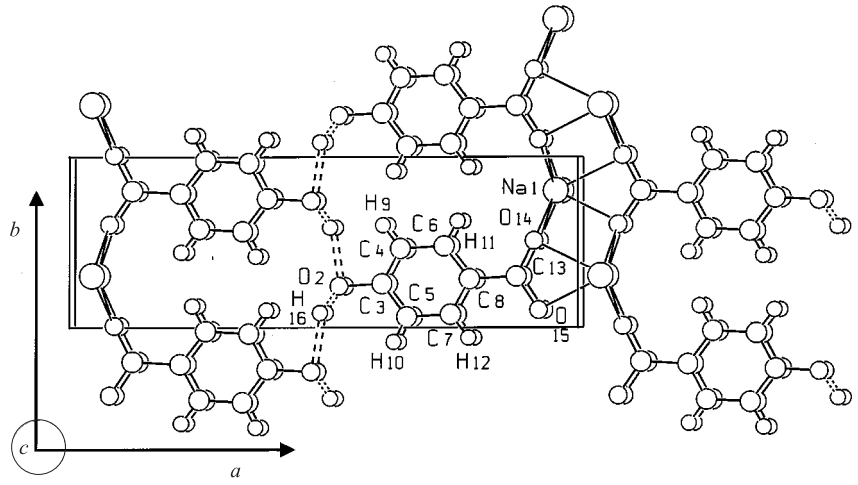

Fig. 4. Packing diagram (*SCAHAKAL*; Keller, 1997) of the layered structure of sodium *para*-hydroxybenzoate in $P2_1$ at $T = 295$ K. The NaO_6 layers are perpendicular to the *a* axis.

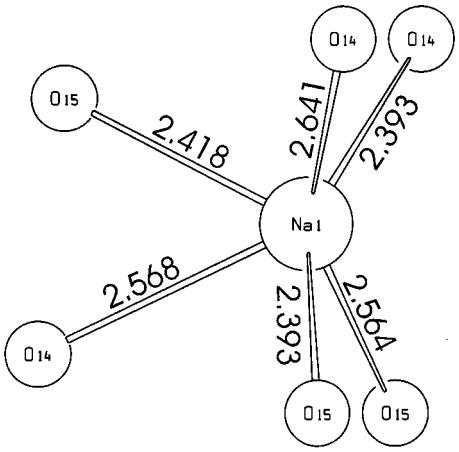

(*a*)

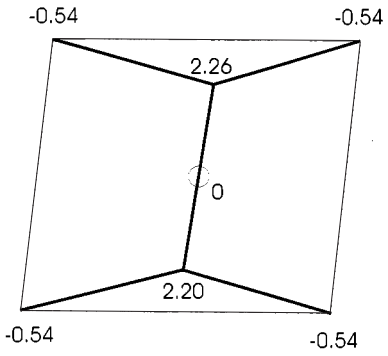

(*b*)

Fig. 5. Coordination polyhedron of sodium in sodium *para*-hydroxybenzoate projected along the *a* axis. (*a*) Bond lengths (Å) between the cation and the oxygen atoms (viewed along the *c* axis). (*b*) Heights (Å) measured from the *bc* plane through the cation.

is supported by the Division of Basic Energy Sciences of the US Department of Energy under grant DE-FG02-86ER45231. Research at the University of Leipzig was supported in part by the Deutsche Forschungsgemeinschaft and the Fond der Chemischen Industrie in Germany. Work at Stony Brook was partially supported by the National Science Foundation under grant DMR 95–01325. Support by the Deutsche Forschungsgemeinschaft (Di 687/2–1) is gratefully acknowledged.

References

Behr, A. (1985). *Chem. Ing. Tech.* **57**, 11, 893–903.
Brockhaus ABC Chemie (1971). Vol. 1 A–K, p. 565. Leipzig: VEB, F. A. Brockhaus Verlag.
Cascarano, G., Favia, L. & Giacovazzo, C. (1992). *J. Appl. Cryst.* **25**, 310–317.
Colapietro, M. & Domenicano, A. (1977). *Acta Cryst.* B**33**, 2240–2243.
Colapietro, M. & Domenicano, A. (1978). *Acta Cryst.* B**34**, 3277–3280.
Colapietro, M., Domenicano, A. & Ceccarini, G. P. (1979). *Acta Cryst.* B**35**, 890–894.
Colapietro, M., Domenicano, A. & Marciante, C. (1979). *Acta Cryst.* B**35**, 2177–2180.
Dinnebier, R. E., Pink, M., Sieler, J. & Stephens, P. W. (1997). *Inorg. Chem.* **36**, 3398–3401.
Finger, L. W., Cox, D. E. & Jephcoat, A. P. (1994). *J. Appl. Cryst.* **27**, 892–900.
Hales, J. L., Jones, J. I. & Lindsey, A. S. (1954). *J. Chem. Soc.* pp. 3145–3151.
Harris, K. D. M. & Tremayne, M. (1996). *Chem. Mater.* **8**, 2554–2570.
Heath, E. A., Singh, P. & Ebisuzaki, Y. (1992). *Acta Cryst.* C**58**, 1960–1965.
Jörchel, P. & Sieler, J. (1994). *Z. Anorg. Allg. Chem.* **620**, 1058–1062.
Keller, E. (1997). *SCHAKAL*97. Kristallographisches Institut der Universität, Freiburg, Germany.
Kolbe, H. J. (1874). *Prak. Ch.* **118**, 107.
Kolbe, H. J. & Lautemann, E. (1860). *Liebigs Ann. Chem.* **115**, 157.
Kunert, M., Dinjus, E., Nauck, M. & Sieler, J. (1997). *Chem. Ber.* **130**, 1461–1465.
Langford, I. & Louër, D. (1996). *Rep. Prog. Phys.* **59**, 131.
Larson, A. C. & Von Dreele, R. B. (1994). *GSAS.* Los Alamos National Laboratory Report LAUR 86–748. (Used version: August 1997.)
Le Bail, A. (1992). *Accuracy in Powder Diffraction II: Proceedings of the International Conference*, May 26–29 1992, edited by E. Prince & J. K. Stalick, NIST Special Publication 846, pp. 142–153. Washington, DC: US Government Printing Office.
Le Bail, A., Duroy, H. & Fourquet, J. L. (1988). *Mater. Res. Bull.* **23**, 447–452.
Lengauer, C. L., Tillmans, E., Zemann, J. & Robert, J.-L. (1995). *Z. Kristallogr.* **210**, 656–661.
Lightfoot, P., Metha, M. A. & Bruce, P. G. (1993). *Science*, **262**, 883–885.
Lindsey, A. S. & Jeskey, H. (1957). *Chem. Rev.* **57**, 583–620.
Manojlovic, L. (1968). *Acta Cryst.* B**24**, 326–330.
Masciocchi, N. & Sironi, A. (1997). *J. Chem. Soc. Dalton Trans.* pp. 4643–4650.
Mehrotra, B. N., Hahn, Th., Eysel, W., Röpke, H. & Illguth, A. (1978). *N. Jahrb. Miner. Monatsh. H*, **9**, 408–421.
Poojary, D. M. & Clearfield, A. (1997). *Acc. Chem. Res.* **30**, 414–422.
Popa, N. C. (1998). *J. Appl. Cryst.* **31**, 176–180.
Rietveld, H. M. (1969). *J. Appl. Cryst.* **2**, 65–71.
Rodríguez-Carvajal, J. (1990). *Abstracts of the Satellite Meeting on Powder Diffraction of the XV Congress of the IUCr*, Toulouse, France, p. 127.
Rodríguez-Carvajal, J., Fernández-Díaz, M. T. & Martínez, J. L. (1991). *J. Phys. Condens. Matter*, **3**, 3215–3234.
Sakakibara, T. & Haraguchi, K. (1980). *Bull. Chem. Soc. Jpn*, **53**, 279–280.
Schmidt, M. W., Finger, L. W., Angel, R. J. & Dinnebier, R. E. (1998). *Am. Mineral.* **83**, 881–888.

Smith, G. S., Johnson, Q. C., Smith, D. K., Cox, D. E. & Zalkin, A. (1988). *Solid State Commun.* **67**, 491–494.
Stephens, P. W. (1999). *J. Appl. Cryst.* **32**, 281–289.
Thompson, P., Cox, D. E. & Hastings, J. B. (1987). *J. Appl. Cryst.* **20**, 79–83.
Thompson, P., Reilly, J. J. & Hastings, J. B. (1987). *J. Less Common Met.* **129**, 105–114.
Ungar, T. & Tichy, G. (1999). *Phys. Status Solidi A*, **171**, 425–434.
Visser, J. W. (1969). *J. Appl. Cryst.* **2**, 89–95.
Von Dreele, R. B. (1998). Personal communication.